

Extreme Variability in a Long Duration Gamma-ray Burst Associated with a Kilonova

P. VERES,^{1,2} P. N. BHAT,² E. BURNS,³ R. HAMBURG,⁴ N. FRAIJA,⁵ D. KOCEVSKI,⁶ R. PREECE,² S. POOLAKKIL,^{1,2}
N. CHRISTENSEN,⁷ M. A. BIZOUARD,⁷ T. DAL CANTON,⁴ S. BALA,⁸ E. BISSALDI,^{9,10} M. S. BRIGGS,^{1,2}
W. CLEVELAND,⁸ A. GOLDSTEIN,⁸ B. A. HRISTOV,² C. M. HUI,¹¹ S. LESAGE,^{1,2} B. MAILYAN,¹² O. J. ROBERTS,¹³ AND
C. A. WILSON-HODGE¹¹

¹*Department of Space Science, University of Alabama in Huntsville, Huntsville, AL 35899, USA*

²*Center for Space Plasma and Aeronomic Research, University of Alabama in Huntsville, Huntsville, AL 35899, USA*

³*Department of Physics & Astronomy, Louisiana State University, Baton Rouge, LA 70803, USA*

⁴*Université Paris-Saclay, CNRS/IN2P3, IJCLab, 91405 Orsay, France*

⁵*Instituto de Astronomía, Universidad Nacional Autónoma de México, Circuito Exterior, C.U., A. Postal 70-264, 04510, CDMX, Mexico*

⁶*NASA Marshall Space Flight Center, Martin Rd. SW, Huntsville, 35808, AL, USA*

⁷*Université Côte d'Azur, Observatoire de la Côte d'Azur, CNRS, Artemis, Nice 06300, France*

⁸*Science and Technology Institute, Universities Space Research Association, Huntsville, AL 35805, USA*

⁹*Dipartimento Interateneo di Fisica, Politecnico di Bari, Via E. Orabona 4, 70125, Bari, Italy*

¹⁰*INFN - Sezione di Bari, Via E. Orabona 4, 70125, Bari, Italy*

¹¹*ST12 Astrophysics Branch, NASA Marshall Space Flight Center, Huntsville, AL 35812, USA*

¹²*Department of Aerospace, Physics and Space Sciences, Florida Institute of Technology, Melbourne, FL 32901, USA*

¹³*Science and Technology Institute, Universities Space and Research Association, 320 Sparkman Drive, Huntsville, AL 35805, USA.*

ABSTRACT

The recent discovery of a kilonova from the long duration gamma-ray burst, GRB 211211A, challenges classification schemes based on temporal information alone. Gamma-ray properties of GRB 211211A reveal an extreme event, which stands out among both short and long GRBs. We find very short variations (few ms) in the lightcurve of GRB 211211A and estimate ~ 1000 for the Lorentz factor of the outflow. We discuss the relevance of the short variations in identifying similar long GRBs resulting from compact mergers. Our findings indicate that in future gravitational wave follow-up campaigns, some long duration GRBs should be treated as possible strong gravitational wave counterparts.

Keywords: gamma rays: individual (211211A)

1. INTRODUCTION

Gamma-ray bursts (GRBs) are typically classified into long or short groups based on the duration of the active gamma-ray episode. Such a classification has historical origins (Kouveliotou et al. 1993), and the physical understanding behind this picture has matured over the following decades: short GRBs (sGRBs) are predominantly from binary neutron star mergers (Duncan & Thompson 1992; Usov 1992; Thompson 1994; Goldstein et al. 2017; Abbott et al. 2017) or possibly from black hole - neutron star mergers (Narayan et al. 1992), while long GRBs (LGRBs) originate from the core collapse of massive stars (Woosley 1993; Paczyński 1998; MacFadyen & Woosley 1999; Woosley & Bloom 2006). There is an overlap between the duration distributions of short and long classes. For this reason, the classification based on the burst duration is complemented by rudimentary spectral information, the hardness ratio

(HR), available for all GRBs. Classifications based on two parameters provide better separation between the classes. On average, sGRBs are harder, while LGRBs are softer (Paciesas et al. 1999; Bhat et al. 2016; von Kienlin et al. 2020). In some cases even two parameters are not sufficient to derive a reliable classification and further observations are needed to hone in on the physical origin of the GRBs (see e.g. the Type I/II classification scheme by Zhang et al. (2009) and refer to Kann et al. (2011) for a discussion of controversial scenarios). LGRBs also include Ultra-long GRBs (ULGRBs) with a duration longer than thousands of seconds (Gendre et al. 2013; Levan et al. 2014; Piro et al. 2014; Greiner et al. 2015; Kann et al. 2018), and LGRBs associated with Supernovae (SNe) Ic (Hjorth et al. 2003). Additionally giant flares from extragalactic magnetars (Roberts et al. 2021) can masquerade as sGRBs at a rate of approxi-

mately one event per year (Burns et al. 2021) further complicating the picture.

At first glance, GRB 211211A is a bright, but otherwise typical LGRB suggesting a collapsar origin, based on the gamma-ray properties. However, Rastinejad et al. (2022); Troja et al. (2022) report a possible kilonova counterpart to GRB 211211A suggesting a compact merger origin, at odds with the gamma-ray classification. GRB 211211A represents one of the clearest breaks with the usual short/long classification. Some sGRB pulses are followed by a longer, extended gamma-ray emission, without associated supernovae (Gehrels et al. 2006). It is possible that GRB 211211A also belongs to this class.

One of the most intriguing features of GRBs is the short variations in their lightcurves. The observed variability could originate from the variations in the central engine with contributions from the jet interacting with the progenitor (Sari & Piran 1997a; Morsony et al. 2010). This variability is imprinted on the emission processes (e.g. internal shocks Sari & Piran 1997b), or alternatively can be ascribed to intrinsic variations in the emitting volume (e.g. by turbulence Narayan & Kumar 2009). Typical variations can be as short as 10 ms, with a handful of examples of sub 10 ms variability. The most extreme case for a GRB is a $\sim 200 \mu\text{s}$ variation (Bhat et al. 1992). On average, sGRBs have shorter variability than LGRBs (Bhat et al. 2012; Golkhou et al. 2015a). The variability timescale constrains the size of the emitting region based on causality arguments (Rybicki & Lightman 1979).

Here, we place GRB 211211A in the context of *Fermi* Gamma-ray Burst Monitor (GBM) GRBs and report on the implications for future gravitational wave (GW) or kilonova searches associated with GRBs. We provide a detailed analysis of the gamma-ray lightcurve highlighting the extreme variability and discuss this the possible association of this GRB with the class of short GRBs with extended emission.

We present gamma-ray observations of GRB 211211A in Section 2, focusing on the minimum variability timescale (Section 3). We present GRB 211211A as a GRB with extended emission, and provide physical parameters of the outflow in Section 4. We end with discussing our results in Section 5. We use the $Q_x = Q/10^x$ convention in c.g.s. units for quantity Q and refer to physical constants using their common notations.

2. DATA ANALYSIS

GRB 211211A (Mangan et al. 2021) triggered *Fermi*-GBM (Meegan et al. 2009) at 13:09:59.65 UT on December 11th, 2021 (T_0). It showed significant emission in all

12 of GBM’s NaI and both the BGO detectors, up to an energy ~ 20 MeV. At trigger time the location of the GRB was outside of the LAT field of view, however Mei et al. (2022) reported detection of photons in the GeV range at $\sim T_0 + 10^4$ s. Swift-BAT (D’Ai et al. 2021), CALET (Tamura et al. 2021), INTEGRAL-SPI/ACS (Minaev et al. 2021) and Insight-HXMT (Zhang et al. 2021) also detected GRB 211211A.

The duration $T_{90} = 34.3 \pm 0.6$ s calculated as the central 90th percentile of the cumulative energy flux in the 50-300 keV range using the *RMfit*¹ software. The hardness ratio over the T_{90} duration, defined as the ratio of fluxes between 50-300 keV and 10-50 keV energy ranges is $HR = 0.850 \pm 0.015$. These two parameters place GRB 211211A on the duration-hardness plane with high probability in the long population (Rastinejad et al. 2022; Bhat et al. 2016; von Kienlin et al. 2020; Rouco Escorial et al. 2021). For spectral analysis we use NaI detectors n2 and na and BGO detector b0. For temporal analysis we can use additional NaI detectors with significant flux: n0, n1, n2, n5, n9, na and nb.

2.1. Lightcurve

Morphologically, the lightcurve can be separated into three parts. This GRB starts with a brief standalone pulse, a precursor, lasting about 0.2 s. Interestingly Xiao et al. (2022), reported tentative quasi-periodic oscillations for this pulse. The second part is the brightest and we refer to it as *the main emission* episode. It starts at T_0+1 s and lasts until T_0+13 s. It consists of a large number of short peaks. The third part starts around T_0+13 s, and we refer to it as *late emission*. It contains less variability than the main emission, it can be detected until about T_0+70 s and it fades smoothly into the background (see Figure 1).

Taken by itself, with duration of ≈ 10 s, even the *main emission* episode would be classified as a LGRB. It is significantly longer than the $\approx 4 - 5$ s limit separating the short and long classes of GBM (von Kienlin et al. 2020). This limit represents the duration of equal probability between the long and short classes when we model the duration distribution using two log-normal components (see e.g. section 4.4 and the associated figure).

2.2. Spectrum

To compare GRB 211211A with other GRBs, we perform a spectral analysis of the brightest peak and the time integrated emission. We note that the time integrated analysis, with fluence $F = (5.1 \pm 0.1) \times 10^{-4}$ erg cm^{-2} does not capture the evolving trends

¹ <https://fermi.gsfc.nasa.gov/ssc/data/analysis/rmfit>

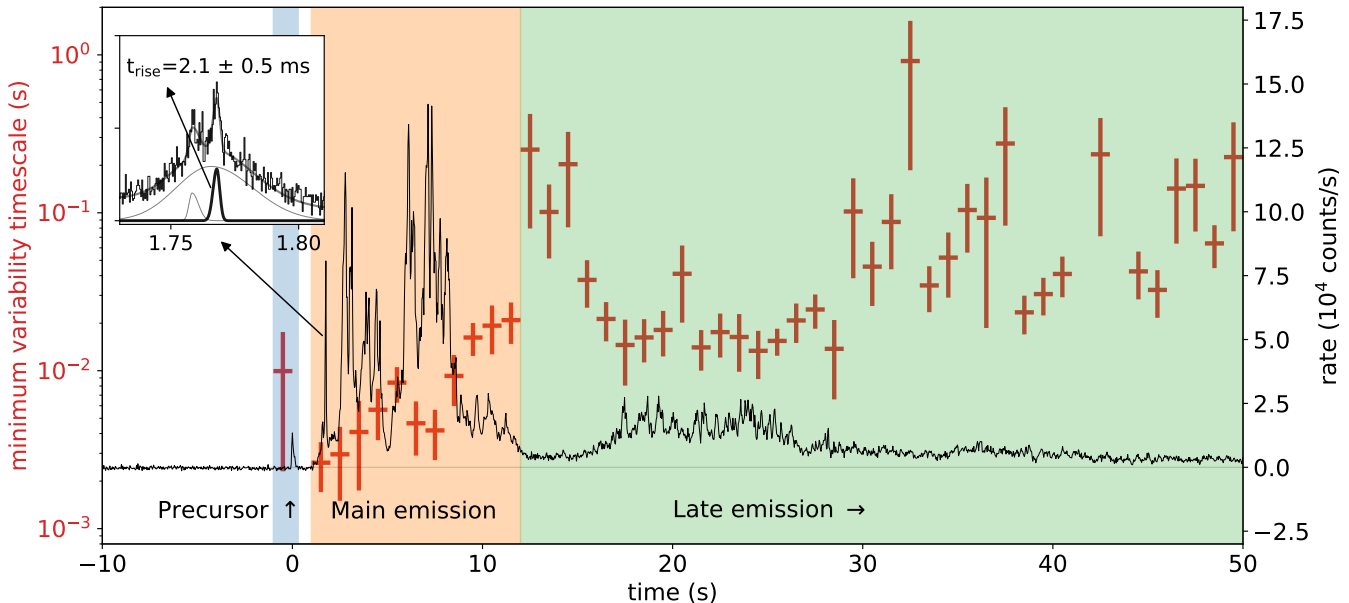


Figure 1. Lightcurve of GRB 211211A (black) and the corresponding minimum variability timescale (red). Inset: Zoomed lightcurve around the time of the shortest variation. Individual pulse models are indicated, with the shortest rise time highlighted in bold.

observed in this burst by e.g. [Gompertz et al. \(2023\)](#) but it is suitable to determine the gamma-ray energetics. The peak flux, commonly reported on 64 ms (sGRBs) and 1.024 s (lGRBs) timescales is $P_{64\text{ms}} = (1.49 \pm 0.02) \times 10^{-4} \text{ erg cm}^{-2} \text{ s}^{-1}$ and $P_{1\text{s}} = (8.10 \pm 0.04) \times 10^{-5} \text{ erg cm}^{-2} \text{ s}^{-1}$, respectively. Both the time integrated and the peak spectra are best fit by Band functions ([Band et al. 1993](#)) with parameters presented in Table 2.

The redshift reported for the host galaxy is $z=0.076$ ([Malesani et al. 2021](#)), corresponding to a luminosity distance of $D_L=346 \text{ Mpc}$ (using $\Omega_m = 1 - \Omega_\Lambda = 0.315$ and $H_0 = 67.4 \text{ km s}^{-1} \text{ Mpc}^{-1}$ ([Planck Collaboration et al. 2020](#))). The isotropic-equivalent gamma-ray energy of GRB 211211A calculated in the 1-10,000 keV range is $E_{\text{iso}} \approx 1.3 \times 10^{52} \text{ erg}$, the peak luminosity, calculated on a 64 ms and 1.024 s timescale is $L_{\text{iso},64\text{ms}} \approx 5.9 \times 10^{51} \text{ erg s}^{-1}$ and $L_{\text{iso},1\text{s}} \approx 2.3 \times 10^{51} \text{ erg s}^{-1}$ respectively (see Table 2).

2.3. GRB 211211A in context of other GRBs

GRB 211211A has higher energy fluence (units of erg cm^{-2}) than all but 4 GRBs in the GBM catalog ([von Kienlin et al. 2020](#)) (GRBs 130427A, 161625B, 171010A and 160821A), corresponding to 99.9th percentile among Fermi GBM GRBs ([Poolakkil et al. 2021](#)). The peak energy flux (units of $\text{erg cm}^{-2} \text{ s}^{-1}$) of GRB 211211A calculated for the brightest 64 ms is brighter than all short GRBs in the catalog. The 1.024 s peak energy flux of GRB 211211A is brighter than all but two long

GRBs prior to GRB 211211A (GRB 130427A ([Preece et al. 2014](#)), and GRB 131014A ([Guiriec et al. 2015](#))).

During the writing of this paper, *Fermi*-GBM detected GRB 221009A ([Lesage et al. 2023](#)) and GRB 230307A ([Dalessi & Fermi GBM Team 2023b](#)) with peak fluxes and fluence larger than GRB 211211A. While GRB 221009A is clearly not from a compact binary merger ([Fulton et al. 2023](#)), GRB 230307A does bear some resemblance to GRB 211211A (see section 4.5).

The peak energy (E_{peak}) measured for the brightest 1 s (1030 keV) is 94.9 percentile among lGRBs and 84.9 percentile among sGRBs.

We conclude that GRB 211211A is at the bright end of peak flux and fluence distributions among both short and the long classes, making it an exceptional GRB in the Fermi GBM sample.

3. MINIMUM VARIABILITY TIMESCALE

The minimum variability timescale (MVT) of a GRB lightcurve represents the shortest timescales, at which coherent changes can be identified. In practice it coincides with the typical timescale (e.g. the rise time) of the shortest pulse in the lightcurve. There are multiple mathematical methods in the literature to derive the MVT. Here we use the methods of [Bhat et al. \(2012\)](#); [Bhat \(2013\)](#) and [Golkhou et al. \(2015a\)](#), but see also [MacLachlan et al. \(2013\)](#).

We binned our lightcurve to 100 μs and searched for the shortest coherent variations. The variability using

the method of [Bhat et al. \(2012\)](#) is $\Delta t_{\text{var}} = 2.6 \pm 0.9$ ms. The [Golkhou et al. \(2015b\)](#) method gives a variability of $\Delta t_{\text{var}} = 2.5 \pm 0.8$ ms. The two methods are independent, and they give consistent MVT values, strengthening the confidence that this is indeed the minimum variability timescale of this burst.

In addition, we identify a pulse with rise time of ≈ 2 ms in Figure 1 (inset) that determines the MVT: we fit the high resolution (400 μ s) lightcurve in the range 1.73 to 1.81 s, (region of the lightcurve where the variability time is the shortest) with the pulse model of [Norris et al. \(2005\)](#), using 3 pulses plus a long term emission modeled as a first degree polynomial. The rise time of the shortest pulse is consistent with minimum variability timescale, as expected ([Bhat et al. 2012](#)). This ~ 2 ms timescale is significantly lower than the 16 ms variability reported by [Yang et al. \(2022\)](#) and the 10 ms reported by [Xiao et al. \(2022\)](#)

We also performed a time resolved variability analysis. We calculate the MVT in each 1 s bin (Figure 1) and find that the separation of the lightcurve into *main* and *late* emission is also reflected in the evolution of the variability timescale: the main emission episode has a clearly shorter variability than the late emission.

3.1. Long duration GRBs with short MVT

GRB 211211A, with $\text{MVT} \sim 2.5$ ms is a clear outlier in the distribution of the MVTs presented in [Golkhou et al. \(2015a\)](#) (see Figure 2, where we plot MVT values that have an uncertainty smaller than the value itself). We have searched for other GRBs that have long duration ($T_{90} \gg 2$ s), and short variability. The sample of [Golkhou et al. \(2015a\)](#) contained MVT values only until 2012. We extended their sample with bursts up to 2022, by additional 2124 *Fermi*-GBM GRBs.

Because the MVT calculation depends on multiple input parameters, that can affect the final value (e.g. detector selection, background, foreground interval, method, etc.), we allow a limit of $\text{MVT} < 15$ ms and $T_{90} > 5$ s in searching for GRB similar to GRB 211211A (see Figure 2).

Applying the above limit, we found 10 potentially interesting GRBs in our sample (see Figure 2). Many of the selected bursts are known, bright GRBs with associated supernovae (e.g. GRB 130427A ([Preece et al. 2014](#)) and GRB 190114C ([Ajello et al. 2020](#))), or their lightcurve does not resemble that of GRB 211211A. We inspected each GRB lightcurve visually, looking for similar lightcurve morphology to GRB 211211A, namely an initial bright, variable phase followed by a longer, less luminous emission episode. After visual inspection of the candidates, we find 3 additional cases with similar

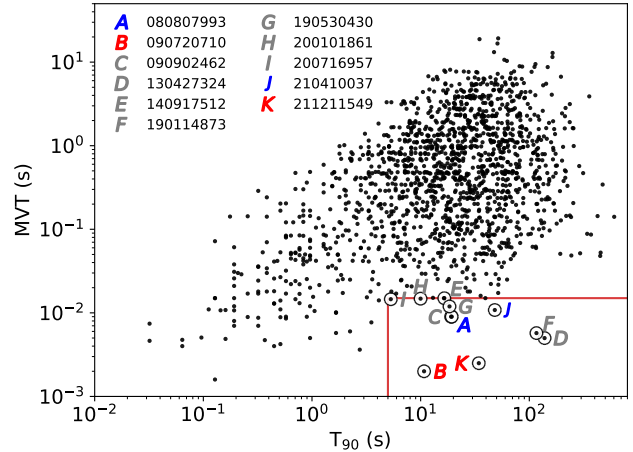


Figure 2. MVT values as a function of T_{90} for all *Fermi*-GBM GRBs with well measured T_{90} and MVT. We highlight GRBs with $T_{90} > 5$ s and $\text{MVT} < 15$ ms (red line) by displaying the GBM trigger number in the legend. GRB 211211A and GRB 090720B are indicated by red letters (**B**, **K**), blue letters (**A**, **J**) mark two possibly similar GRBs, but with higher MVT, other selected GRBs have gray letters.

GRB	T_{90} (s)	MVT(s)
120712571	22.528 ± 5.431	0.6646 ± 0.1799
120716577	24.960 ± 3.958	7.7225 ± 1.8755
120728934	32.768 ± 2.429	1.5558 ± 0.6006
120805706	1.856 ± 1.296	0.6957 ± 0.1710
120806007	26.624 ± 1.557	0.2707 ± 0.1133
120811014	0.448 ± 0.091	0.0182 ± 0.0066

Table 1. Table of MVT values for GBM GRBs. The table contains GRBs starting from the end of GRBs covered in [Golkhou et al. \(2015a\)](#). The table is available in its entirety in machine-readable form.

lightcurves as GRB 211211A. Among these three, only GRB 090720B has comparable variability timescale (~ 2 ms), while other similar GRBs: 210410A and 080807 have ~ 10 ms variability. We thus conclude that bursts with long duration and short variability are rare, especially those GRBs that exhibit a short pulse followed by softer, extended emission. We further conclude that GRB 211211A lies at the extreme low end of the variability timescale distribution of *Fermi*-GRBs.

4. RESULTS

4.1. GRB 211211A as a short GRB with extended emission

GRB 060614 ([Gehrels et al. 2006](#)), a nearby long event with duration in excess of 100 s has no supernova

Table 2. Spectral parameters of GRB 211211A

Time (s)	E_{peak}	α	β	Energy Flux	Fluence	L_{iso}	E_{iso}
$T-T_0$ (s)	keV			10^{-5} erg cm^{-2} s^{-1}	10^{-5} erg cm^{-2}	10^{51} erg s^{-1}	10^{52} erg
0-52.2	$545^{+12.3}_{-10.8}$	$-1.180^{+0.005}_{-0.006}$	$-2.13^{+0.02}_{-0.019}$	-	50.7 ± 0.1	-	1.25 ± 0.003
7.104-7.168	1737^{+114}_{-121}	$-0.878^{+0.019}_{-0.020}$	$-2.90^{+0.26}_{-0.19}$	14.9 ± 0.2	-	5.89 ± 0.09	-
7.168-8.192	1033^{+27}_{-31}	$-0.941^{+0.008}_{-0.008}$	$-2.72^{+0.07}_{-0.06}$	8.10 ± 0.04	-	2.33 ± 0.01	-

NOTE—Spectral parameters for GRB 211211A fitting a Band function and using the standard time intervals: the entire GRB, brightest 1024 ms and 64 ms. The flux and fluence are reported in the 10-1,000 keV range. L_{iso} and E_{iso} are reported in the 1-10,000 keV (observer) range.

detection to deep limits, indicating a possible merger origin. Its lightcurve morphology, a short pulse, followed by extended emission established a new category of GRBs (sGRB-EE). GRB 060614 was detected by Swift-BAT. For this GRB we derive an MVT value of $\Delta t_{\text{var}} = 36 \pm 4$ ms. [Rastinejad et al. \(2022\)](#); [Gompertz et al. \(2023\)](#); [Xiao et al. \(2022\)](#); [Troja et al. \(2022\)](#) find that GRB 211211A has broadly consistent properties with other sGRB-EE GRBs. We also find that GRB 211211A has consistent features with sGRB-EE. The time-resolved MVT (Figure 1) also clearly delineates the sGRB and the extended emission.

[Kaneko et al. \(2015\)](#) considered a sample of sGRB-EE in the *Fermi*-GBM sample. We extend their list (see Table 3) and investigate the variability timescale of sGRB-EE (Burns et al. in preparation). We find that GRB 211211A has shorter variability timescale than all the GBM sGRB-EE. This means that the MVT of GRB 211211A is extreme also among the short GRBs with extended emission (including the archetypal GRB 060614). We also note that the MVT of GRB 211211A is close to the short end of even the short duration GRBs (see Figure 2).

4.2. Possible afterglow origin of the late emission

As noted in the previous section, GRB 211211A fits into the category of short GRB with extended emission ([Gehrels et al. 2006](#); [Norris et al. 2010](#)). The *main emission* plays the role of the short GRB, and the *late emission* episode corresponds to the extended emission.

The origin of the extended emission is unclear, sometimes it is associated with late energy injection into the GRB (e.g. [Bucciantini et al. 2012](#)). In many cases, the extended emission has appreciable variability and for this reason its association with afterglow emission is generally disfavored ([Norris & Bonnell 2006](#)). Based on the fact that the *late emission* (T_0+12 to T_0+70 s in Figure 1) has longer variability timescale than the *main emission*, we explore the afterglow origin for the *late emis-*

Trigger number	MVT (ms)	T_{90} (s)
081110601	291 ± 11	11.8 ± 2.6
090227772	~ 5	1.28 ± 1.03
090510016	5 ± 1	0.96 ± 0.14
090831317	15 ± 4	39.4 ± 0.6
100916779	88 ± 8	12.8 ± 2.1
111221739	18 ± 6	27.1 ± 7.2
140819160	43 ± 20	6.7 ± 3.7
170728961	54 ± 15	46.3 ± 0.8
180618030	~ 7	3.7 ± 0.6
190308923	~ 419	45.6 ± 2.83
200219317	~ 55	1.15 ± 1.03
200313456	~ 284	5.2 ± 4.4
201104001	25 ± 8	52.5 ± 7.4

Table 3. Sample of short GRBs with extended emission. Values without errors represent cases where the signal-to-noise wasn't sufficient to determine an error.

sion. In this scenario the late emission is emitted by the shocked circumstellar medium as it slows down the shells that were responsible for the prompt emission. Detecting the afterglow in the γ -ray regime has been reported before (e.g. [Giblin et al. 1999](#); [Connaughton 2002](#); [Ajello et al. 2020](#)) and it is common for bright GRBs.

Early afterglow lightcurves, especially in X-ray and GeV sometimes show a rising phase, peak and a decay representing the onset of the afterglow. Here the peak marks the deceleration time. We binned the GBM lightcurve from 13 to 70 s after the trigger into bins with signal to noise ratio of 60. We fit each spectrum with a Comptonized function (power law with exponential cutoff) and calculate the flux density at 10 keV (see Figure 3). The flux evolution shows a clear peak. We fit the flux density curve with a smoothly broken power law function, $f(t) \propto [(t/t_{\text{peak}})^{s\alpha_{\text{rise}}} + (t/t_{\text{peak}})^{s\alpha_{\text{decay}}}]^{-1/s}$, where s is the smoothness parameter, fixed here to 1. We find the index of the rising phase $\alpha_{\text{rise}} = 2.0 \pm 0.3$ consistent with the expectation of $\alpha_{\text{rise}} = 2$ if it originates

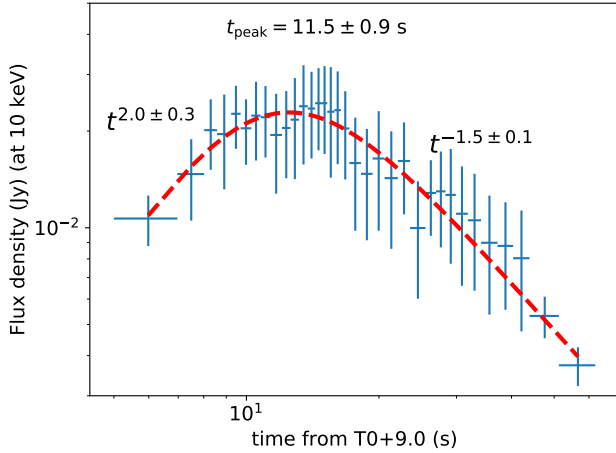


Figure 3. Flux density evolution of the late emission, fit with a smoothly broken power law. The time axis is shifted by 9 s with respect to the trigger time to match the end of the main episode.

from the forward shock before deceleration (Sari & Piran 1999). We note that α_{rise} is sensitive to the choice of the zero point. Here we choose $T_0 + 9$ s, because this is the approximate end time of the highly variable, main emission episode. The peak of the flux occurs at 20.5 ± 0.9 s after the trigger time. The temporal decay index after the peak is $\alpha_{\text{decay}} = -1.5 \pm 0.1$, which in the forward shock scenario corresponds to $1/2 - 3p/4$, where p is the index of shocked electron population’s the power law distribution. In our case we get $p = 2.7 \pm 0.1$, which is consistent with the values that are commonly found for afterglows (e.g. Panaitescu & Kumar 2001).

We thus conclude that the afterglow interpretation is possible at least in some cases of GRBs with extended emission.

4.3. Lorentz factor constraints

The Lorentz factor of the outflow is a basic ingredient of the physical picture. We can provide a lower limit on the Lorentz factor if the highly variable prompt gamma-ray lightcurve is produced by internal shocks (Rees & Mészáros 1994). In this scenario the emission radius (R_{IS}) has to be above the photosphere (R_{ph}) where the optical depth is unity. The internal shock radius is $R_{\text{IS}} \approx 2c\Gamma^2\Delta t_{\text{var}}$, while the photosphere radius is $R_{\text{ph}} = L\sigma_T/8\pi m_p c^3\Gamma^3$, assuming the photosphere occurs in the coasting phase (i.e. the jet does not accelerate any more, $\Gamma(R) = \text{constant}$). From $R_{\text{IS}} \gtrsim R_{\text{ph}}$, we have

$$\Gamma \gtrsim 170 \left(\frac{L_{\gamma, 51.8}}{\eta_{\gamma, -0.7}} \right)^{1/5} \left(\frac{\Delta t_{\text{var}}}{2.5 \text{ ms}} \right)^{-1/5}. \quad (1)$$

Meaningful Lorentz factor constraint using this method is only possible for GRBs with high luminosity and short variability, uniquely relevant for GRB 211211A.

We can calculate the bulk Lorentz factor by identifying the peak of Figure 3 with the onset of the afterglow or the deceleration time. The deceleration radius corresponding to the deceleration time (t_{dec}) marks the distance from the central engine where the relativistic outflow has plowed up interstellar matter that is a fraction $\sim 1/\Gamma$ of the jet mass. Using the expression of t_{dec} , the Lorentz factor evolving a constant-density medium will be:

$$\Gamma = \left(\frac{3E_k}{4\pi m_p c^5 n} \right)^{1/8} t_{\text{dec}}^{-3/8} \quad (2)$$

$$\approx 1200 \left(\frac{E_{\gamma, 52.1}}{n_{-4} \eta_{\gamma, -0.7}} \right)^{1/8} \left(\frac{t_{\text{peak}}}{11.5 \text{ s}} \right)^{-3/8}. \quad (3)$$

Here we chose a gamma-ray efficiency of $\eta_{\gamma} = E_{\gamma}/E_k = 7.8\%$, where E_k is the kinetic isotropic equivalent energy, and $n = 10^{-4} \text{ cm}^{-3}$ the constant interstellar number density, as scaling values, from Mei et al. (2022). If we conservatively measure the peak from the trigger time, instead of the 9 s shift that we introduced, the Lorentz factor becomes $\Gamma \approx 980$.

Sonbas et al. (2015) present a correlation between variability timescale and Lorentz factor based on a compilation of Lorentz factor estimates. The relationship they find is $t_{\text{var}}(\Gamma) \propto \Gamma^{-4}$ for $\Gamma \gtrsim 200$ and $t_{\text{var}} \approx \text{constant}$ otherwise. Inverting the correlation, and substituting $\Delta t_{\text{var}} = 2.5$ ms, we get $\Gamma \approx 900$, which is consistent with the above estimates. Furthermore, the Lorentz factor estimates from different methods are consistent with the best estimate by Mei et al. (2022) of $\log \Gamma \approx 3.1_{-0.6}^{+0.9}$. In the internal shock scenario the emission radius of the gamma-rays will be:

$$R_{\gamma} \approx 2\Gamma^2 c \Delta t_{\text{var}} = 1.5 \times 10^{14} \Gamma_3^2 \left(\frac{\Delta t_{\text{var}}}{2.5 \text{ ms}} \right) \text{ cm}. \quad (4)$$

4.4. Event rate: the tail of the merger distribution

The 10 year GBM GRB catalog (von Kienlin et al. 2020) contains in excess of 2300 GRBs with duration measurements. The distribution of the T_{90} durations is modeled as the sum of two log-normal functions. The exact reason why the T_{90} distribution would follow a log-normal distribution is unclear (for a possible explanation see Ioka & Nakamura 2002), and in reality the distributions could be asymmetrical (Tarnopolski 2019). Because the two component model provides a good fit to the distribution, we will consider this description to calculate the rate for mergers masquerading as IGRBs (see Figure 4).

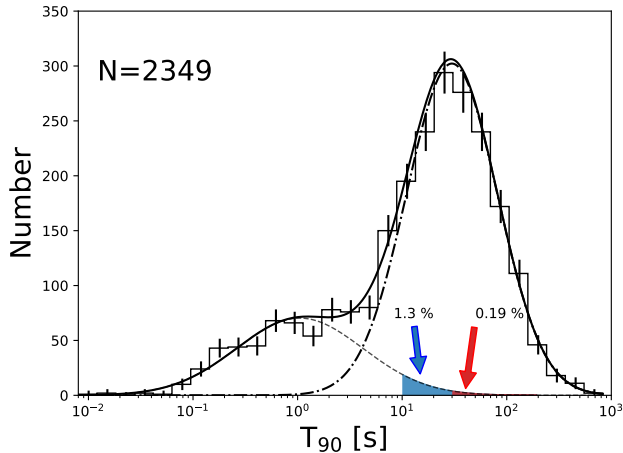


Figure 4. T_{90} distribution of 10 years of GBM GRBs (von Kienlin et al. 2020). Fractions of short GRBs with $T_{90} > 10$ s and $T_{90} > 30$ s are indicated.

We integrate the short model from 10 s, broadly corresponding to the duration of the *main emission* and the actual $T_{90} \sim 10$ s of the similarly short MVT GRB 090720B (Section 4.5). We also integrate the short model component for $T_{90} > 30$ s corresponding roughly to the T_{90} of GRB 211211A. We find about 1.3 % (3 per year) of short *Fermi*-GBM GRBs will have $T_{90} > 10$ s and about 0.19 % (0.4 per year) of short GRBs will have $T_{90} > 30$ s.

4.5. Other examples of long duration and short MVT

GRB 090720B (GBM trigger 090720710, Burgess et al. (2009)) was a bright GRB, with similar properties as GRB 211211A: an initial bright, highly variable set of overlapping pulses, followed by weaker, less variable emission (Figure 5). We cross-check the short variability measurement by Golkhou et al. (2015a), $\Delta t = 2 \pm 1$ ms, and consistently find $\Delta t = 2.6 \pm 0.9$ ms with the method of Bhat et al. (2012). The duration of this GRB is $T_{90} = 10.8 \pm 1.1$ s. Time resolved variability similarly shows a shorter timescale in the main emission compared to the longer lasting episode. GRB 090720B has no redshift measurement, however it is detected by *Fermi*-LAT (Rubtsov et al. 2012; Ajello et al. 2019).

Two further examples with larger variability timescale (~ 10 ms) are GRB 080807 (von Kienlin et al. 2020) and 210410A (Wood et al. 2021) with T_{90} of 19.1 ± 0.2 s and 48.1 ± 2.8 s respectively. Neither have a redshift measurement. Except for GRB 080807, the other 3 selected GRBs have been detected at high energy by LAT. GRB 080807 occurred in a unfavorable geometry for LAT.

GRB 230307A is a recent bright GRB that has tentatively similar properties as GRB 211211A. Despite its long duration ($T_{90} \approx 35$ s, Dalessi & Fermi GBM Team

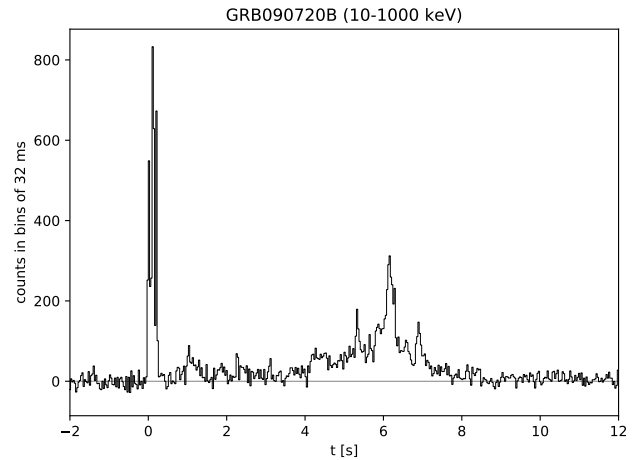


Figure 5. Lightcurve of GRB 090720B with similar short pulse + extended emission structure. GRB 090720B has similarly short (~ 2 ms) variability timescale as GRB 211211A.

(2023b)) it shows short variations like GRB 211211A and has tentative kilonova signature (Levan et al. 2023). Because of its extreme brightness the prompt measurement suffers from instrumental effects (Dalessi & Fermi GBM Team 2023a). A detailed study of GRB 230307A is left for a forthcoming paper.

4.6. Implications for searches for GW counterparts

Having characterized the gamma-ray emission of GRB 211211A, there still remains an intriguing question. How can a merger event give rise to a GRB that has a duration well in excess of the historical 2 s limit between the short and long classes? Even if we place GRB 211211A at a larger distance where only the main emission episode is detectable, its duration will be ~ 10 s and it will be classified as a likely long GRB. This suggests that GRBs with duration $\gtrsim 5$ s can possibly originate from compact binary mergers and be gravitational wave counterparts. Follow-up decisions should consider this fact.

If a sub-class of long GRBs corresponds to compact binary mergers as their source then this will have implications for the gravitational-wave signal search strategy of LIGO-Virgo-KAGRA (LVK). Currently LVK search for gravitational waves in coincidence with GRBs detected by the Fermi and Swift satellites (Abbott et al. 2021, 2022). In these searches, GRBs are classified as short if $T_{90} < 2$ s, long if $T_{90} > 4$ s, or ambiguous for all the other cases. The times coincident with GRBs classified as short or ambiguous are searched for gravitational-wave signals from compact binary mergers using a coherent matched filter analysis, PyGRB (Harry & Fairhurst 2011; Williamson et al. 2014). The merger time is as-

sumed to fall within a $[-5, 1]$ s window, where 0 corresponds to the GRB trigger time.

LVK also use an excess power analysis to search for generic transient signals associated with all GRBs, namely X-Pipeline (Sutton et al. 2010; Was et al. 2012). The search window for gravitational-wave transients begins 600 s before the GRB trigger time, and stops 60 s after trigger time; if $T_{90} > 60$ s then the end of the search window is T_{90} .

During observing run O3, times coincident with 49 GRBs were examined targeting compact binary merger signals. The times coincident with 191 GRBs were examined with the generic search pipeline (Abbott et al. 2021, 2022). If only the GRB T_{90} is considered, as is presently the case for these LVK analyses, then including GRBs such as GRB 211211A will require a significant broadening of the “ambiguous” class, considerably increasing the number of GRBs that will have to be analyzed with the compact binary merger pipeline. This is not an impossible challenge, but would require significantly more human and computing resources, and would increase the chance of a false alarm from the significantly larger sample of GRBs that are not originated by compact binary mergers.

The results of this study motivate the design of a more reliable GRB classification scheme that includes the MVT in addition to T_{90} . The observation of a kilonova should obviously also be incorporated into this improved classification.

5. DISCUSSION AND CONCLUSION

The observation of GRB 211211A represents one of the clearest examples that defy the duration based GRB classification scheme. We analyzed the gamma-ray properties of GRB 211211A in context of the *Fermi*-GBM GRB population. We found that GRB 211211A is one

of the brightest GRBs among both the merger and collapsar population.

We found indications that the extended emission can be modeled as early afterglow in the gamma-rays, and that leads to an estimate of the Lorentz factor. We calculated the variability timescale with different methods and conclusively found one of the shortest variation among long duration GRBs. The short variability has implications on the emission mechanisms and lets us determine the physical parameters of the source. We found the Lorentz factor consistent with $\Gamma \approx 1000$, which puts it among the highest inferred values. $\Gamma \approx 1000$ agrees well with the value reported by Mei et al. (2022) and it is larger than the values (≈ 100) derived by Gompertz et al. (2023); Rastinejad et al. (2022).

We estimated the fraction of short GRBs based on the best fit to the duration distribution. Even though the extrapolation is uncertain, we can conclude that ~ 3.1 GRBs per year with merger origin will have $T_{90} > 10$ s, and 0.44 GRBs per year will have $T_{90} > 30$ s.

The realization that long GRBs can also emanate from binary mergers has profound implications on the follow-up program of future GW observations. First of all, if a GRB presents a spike and extended emission structure, follow-up is warranted. Here we propose that fast variations in the lightcurve may be a distinguishing feature of mergers. It is more likely however that the variations have a continuous distribution and GRB 211211A is special even among the short GRBs with extended emission. Indeed we found that only one long GRB has comparably short MVT. The flux and fluence of GRB 211211A are both extreme among the *Fermi*-GBM GRBs.

Acknowledgements- UAH co-authors acknowledge NASA funding from cooperative agreement 80MSFC22M0004. NF is grateful to UNAM-DGAPA-PAPIIT for the funding provided by grant IN106521. USRA co-authors acknowledge NASA funding from cooperative agreement 80MSFC17M0022.

REFERENCES

- Abbott, B. P., Abbott, R., Abbott, T. D., et al. 2017, *ApJL*, 848, L13
- Abbott, R., et al. 2021, *Astrophys. J.*, 915, 86
- . 2022, *Astrophys. J.*, 928, 186
- Ajello, M., Arimoto, M., Axelsson, M., et al. 2019, *ApJ*, 878, 52
- . 2020, *ApJ*, 890, 9
- Band, D., Mateson, J., Ford, L., et al. 1993, *ApJ*, 413, 281
- Bhat, N. P., Meegan, C. A., von Kienlin, A., et al. 2016, *ApJS*, 223, 28
- Bhat, P. N. 2013, arXiv e-prints, arXiv:1307.7618
- Bhat, P. N., Fishman, G. J., Meegan, C. A., et al. 1992, *Nature*, 359, 217
- Bhat, P. N., Briggs, M. S., Connaughton, V., et al. 2012, *ApJ*, 744, 141
- Bucciantini, N., Metzger, B. D., Thompson, T. A., & Quataert, E. 2012, *MNRAS*, 419, 1537
- Burgess, J. M., Goldstein, A., & van der Horst, A. J. 2009, *GRB Coordinates Network*, 9698, 1
- Burns, E., Svinkin, D., Hurley, K., et al. 2021, *The Astrophysical Journal Letters*, 907, L28
- Connaughton, V. 2002, *ApJ*, 567, 1028

- D’Ai, A., Ambrosi, E., D’Elia, V., et al. 2021, GRB Coordinates Network, 31202, 1
- Dalessi, S., & Fermi GBM Team. 2023a, GRB Coordinates Network, 33551, 1
- . 2023b, GRB Coordinates Network, 33407, 1
- Duncan, R. C., & Thompson, C. 1992, ApJL, 392, L9
- Fulton, M. D., Smartt, S. J., Rhodes, L., et al. 2023, ApJL, 946, L22
- Gehrels, N., Norris, J. P., Barthelmy, S. D., et al. 2006, Nature, 444, 1044
- Gendre, B., Stratta, G., Atteia, J. L., et al. 2013, ApJ, 766, 30
- Giblin, T. W., van Paradijs, J., Kouveliotou, C., et al. 1999, ApJL, 524, L47
- Goldstein, A., Veres, P., Burns, E., et al. 2017, ApJL, 848, L14
- Golkhou, V. Z., Butler, N. R., & Littlejohns, O. M. 2015a, ApJ, 811, 93
- . 2015b, ApJ, 811, 93
- Gompertz, B. P., Ravasio, M. E., Nicholl, M., et al. 2023, Nature Astronomy, 7, 67
- Greiner, J., Mazzali, P. A., Kann, D. A., et al. 2015, Nature, 523, 189
- Guiriec, S., Mochkovitch, R., Piran, T., et al. 2015, ApJ, 814, 10
- Harry, I. W., & Fairhurst, S. 2011, Phys. Rev. D, 83, 084002
- Hjorth, J., Sollerman, J., Møller, P., et al. 2003, Nature, 423, 847
- Ioka, K., & Nakamura, T. 2002, ApJL, 570, L21
- Kaneko, Y., Bostanci, Z. F., Göğüş, E., & Lin, L. 2015, MNRAS, 452, 824
- Kann, D. A., Kloze, S., Zhang, B., et al. 2011, ApJ, 734, 96
- Kann, D. A., Schady, P., Olivares, E. F., et al. 2018, A&A, 617, A122
- Kouveliotou, C., Meegan, C. A., Fishman, G. J., et al. 1993, ApJL, 413, L101
- Lesage, S., Veres, P., Briggs, M. S., et al. 2023, arXiv e-prints, arXiv:2303.14172
- Levan, A. J., Tanvir, N. R., Starling, R. L. C., et al. 2014, ApJ, 781, 13
- Levan, A. J., Gompertz, B. P., Malesani, D. B., et al. 2023, GRB Coordinates Network, 33569, 1
- MacFadyen, A. I., & Woosley, S. E. 1999, ApJ, 524, 262
- MacLachlan, G. A., Shenoy, A., Sonbas, E., et al. 2013, MNRAS, 432, 857
- Malesani, D. B., Fynbo, J. P. U., de Ugarte Postigo, A., et al. 2021, GRB Coordinates Network, 31221, 1
- Mangan, J., Dunwoody, R., Meegan, C., & Fermi GBM Team. 2021, GRB Coordinates Network, 31210, 1
- Meegan, C., Lichti, G., Bhat, P. N., et al. 2009, ApJ, 702, 791
- Mei, A., Banerjee, B., Oganessian, G., et al. 2022, Nature, 612, 236
- Minaev, P., Pozanenko, A., & GRB IKI FuN. 2021, GRB Coordinates Network, 31230, 1
- Morsony, B. J., Lazzati, D., & Begelman, M. C. 2010, ApJ, 723, 267
- Narayan, R., & Kumar, P. 2009, MNRAS, L193+
- Narayan, R., Paczynski, B., & Piran, T. 1992, ApJL, 395, L83
- Norris, J. P., & Bonnell, J. T. 2006, ApJ, 643, 266
- Norris, J. P., Bonnell, J. T., Kazanas, D., et al. 2005, ApJ, 627, 324
- Norris, J. P., Gehrels, N., & Scargle, J. D. 2010, ApJ, 717, 411
- Paciesas, W. S., Meegan, C. A., Pendleton, G. N., et al. 1999, ApJS, 122, 465
- Paczyński, B. 1998, ApJL, 494, L45
- Panaiteescu, A., & Kumar, P. 2001, ApJL, 560, L49
- Piro, L., Troja, E., Gendre, B., et al. 2014, ApJL, 790, L15
- Planck Collaboration, Aghanim, N., Akrami, Y., et al. 2020, A&A, 641, A6
- Poolakkil, S., Preece, R., Fletcher, C., et al. 2021, ApJ, 913, 60
- Preece, R., Burgess, J. M., von Kienlin, A., et al. 2014, Science, 343, 51
- Rastinejad, J. C., Gompertz, B. P., Levan, A. J., et al. 2022, Nature, 612, 223
- Rees, M. J., & Mészáros, P. 1994, ApJL, 430, L93
- Roberts, O. J., Veres, P., Baring, M. G., et al. 2021, Nature, 589, 207
- Rouco Escorial, A., Fong, W., Veres, P., et al. 2021, ApJ, 912, 95
- Rubtsov, G. I., Pshirkov, M. S., & Tinyakov, P. G. 2012, MNRAS, 421, L14
- Rybicki, G. B., & Lightman, A. P. 1979, Radiative processes in astrophysics (New York, Wiley-Interscience, 1979. 393 p.)
- Sari, R., & Piran, T. 1997a, MNRAS, 287, 110
- . 1997b, ApJ, 485, 270
- . 1999, ApJ, 520, 641
- Sonbas, E., MacLachlan, G. A., Dhuga, K. S., et al. 2015, ApJ, 805, 86
- Sutton, P. J., et al. 2010, New J. Phys., 12, 053034
- Tamura, T., Yoshida, A., Sakamoto, T., et al. 2021, GRB Coordinates Network, 31226, 1
- Tarnopolski, M. 2019, ApJ, 870, 105
- Thompson, C. 1994, MNRAS, 270, 480

- Troja, E., Fryer, C. L., O'Connor, B., et al. 2022, *Nature*, 612, 228
- Usov, V. V. 1992, *Nature*, 357, 472
- von Kienlin, A., Meegan, C. A., Paciesas, W. S., et al. 2020, arXiv e-prints, arXiv:2002.11460
- Was, M., Sutton, P. J., Jones, G., & Leonor, I. 2012, *Phys. Rev. D*, 86, 022003
- Williamson, A. R., Biwer, C., Fairhurst, S., et al. 2014, *Phys. Rev. D*, 90, 122004
- Wood, J., Meegan, C., & Fermi GBM Team. 2021, *GRB Coordinates Network*, 29788, 1
- Woosley, S. E. 1993, *ApJ*, 405, 273
- Woosley, S. E., & Bloom, J. S. 2006, *ARA&A*, 44, 507
- Xiao, S., Zhang, Y.-Q., Zhu, Z.-P., et al. 2022, arXiv e-prints, arXiv:2205.02186
- Yang, J., Zhang, B. B., Ai, S. K., et al. 2022, arXiv e-prints, arXiv:2204.12771
- Zhang, B., Zhang, B.-B., Virgili, F. J., et al. 2009, *ApJ*, 703, 1696
- Zhang, Y. Q., Xiong, S. L., Li, X. B., et al. 2021, *GRB Coordinates Network*, 31236, 1